Electron mobility in two-dimensional modulation-doped $In_{1-x}Al_xAs/In_{1-y}Ga_yAs$ alloy systems

J. E. Hasbun
Department of Physics, West Georgia College, Carrollton, Georgia 30118
(Received 8 February 1995; revised manuscript received 10 April 1995)

The electronic mobility is investigated in the two-dimensional modulation-doped $In_{1-x}Al_xAs/In_{1-y}Ga_yAs$ alloy system using a memory-function theoretical framework. A variational wave-function model with penetration into the barrier side of the heterostructure is employed in order to facilitate the use of analytic matrix elements for the various scattering mechanisms. Scattering due to polar optical (Frolich coupling, deformation potential), acoustic (deformation potential), impurities (remote and background), interface roughness, and alloy fluctuations are included in the calculations. The parameters used here are obtained within the virtual crystal approximation appropriate to the compositions x and y studied in conjunction with the parameters for the parent compounds. The mobility results obtained versus temperature are compared with experimental data for the above system.

I. INTRODUCTION

Mobilities in two-dimensional (2D) electron-gas systems have been intensively studied, experimentally and theoretically, ever since the modulation-doping technique was used in conjunction with the molecular-beam epitaxy technology[1] in order to grow high quality 2D structures.

The $In_{1-y}Ga_yAs$ material based 2D structures are of importance in high-speed field-effect transistor applications.[2–9] Electron mobilities in $Al_yGa_{1-y}As/In_{1-x}Ga_xAs$ quantum-well structures have been studied theoretically,[2] using the Boltzmann transport approach. In this work, experimental measurements were also made. Monte Carlo studies of the transient transport and high-field velocity characteristics of $Ga_yIn_{1-y}As/Al_xIn_{1-x}As$ 2D systems have demonstrated the importance of these structures.[4] High electron-gas mobilities in $In_{1-y}Ga_yAs$-InP had been reported in the early 80's (Ref. 9) and transport phenomena in an $In_{1-y}Ga_yAs/In_{1-y}Al_xAs$ field-effect transistor[3] give further evidence of the significance of $In_{1-y}Ga_yAs$ based electron-gas systems.

In the present work, the electronic mobility in the modulation-doped $In_{1-x}Al_xAs/In_{1-y}Ga_yAs$ alloy heterojunction system is investigated within a memory-function approach. This theoretical technique has its roots in the work of Lei and Ting,[10] who conducted a study of nonlinear electron transport for a system of electrons interacting with impurities and phonons. Here, the authors[10] made use of a Hamiltonian, wherein the coordinates that describe the motion of the electrons' center of mass is separated from the coordinates that describe the electrons' relative motion.[11] Ting and Nee[12] showed how the memory function[13] can be obtained from such Hamiltonian. Our work[14] has employed the above method[10–12] in studies of transport in a $GaAs/Al_xGa_{1-x}As$ 2D heterojunction system in a one subband model. Further work using a similar approach as well as the memory-function approach has been carried out recently.[15]

Previous studies using the present theoretical technique,[10–12] in 2D systems, employed a Hamiltonian that included scattering, due to impurities and phonons only.[14–17] In contrast, the present study extends the earlier work[14] to include, in addition, interface roughness[5,18] and alloy scattering[6,7] contributions. Moreover, in this work, the heterojunction potential for the $In_{1-x}Al_xAs/In_{1-y}Ga_yAs$ system is modeled by the use of Ando's self-consistent wave-function method[19] in conjunction with the virtual-crystal approximation (VCA).[20] This allows the representation of the system's properties, for specific alloy concentrations x and y, with the help of the parent compounds' known parameters. Below, in Sec. II, the model is presented, in Sec. III, the outline of the calculation is given and the various matrix elements employed are discussed. The results are presented in Sec. IV, followed by the conclusion in Sec. V.

II. MODEL

A. Self-consistent heterojunction potential

The heterojunction potential used here is based on the work of Ando.[19] The electrons are described by a ground-state wave function of the form

$$\psi_k(r,z)=(1/A)^{1/2}\exp[i(k\cdot r)]\zeta(z)\ , \tag{2.1a}$$

with associated energy level

$$E_k=E_0+\frac{\hbar^2k^2}{2m_A}\ , \tag{2.1b}$$

where E_0 is the energy of the ground state and $\mathbf{k}=(k_x,k_y)$ is a two-dimensional wave vector that describes the free-electron motion in the x,y plane. The envelope, $\zeta(z)$, describes the localization of the electrons in the z direction perpendicular to the interface between the barrier material, $In_{1-x}Al_xAs$ (B), and the channel material, $In_{1-y}Ga_yAs$ (A). The mass, m_A, is the electronic effective mass of the A material ($In_{1-y}Ga_yAs$) for concentration y.

The envelope, $\zeta(z)$, is given by

$$\zeta(z)=\begin{bmatrix}\zeta_A(z)\equiv Bb^{1/2}(bz+\beta)\exp(-bz/2), & z>0\\ \zeta_B(z)\equiv B'(b')^{1/2}\exp(b'z/2), & z<0\end{bmatrix}, \tag{2.2}$$

where b and b' are variational parameters. The quantities B, B', and β are given in terms of b and b' by

$$B=[\beta^2(1+t_{11}^2 b/b')+2\beta+2]^{-1/2},$$
$$B'=(b/b')^{1/2}\beta t_{11}B, \tag{2.3a}$$

with

$$\beta=2bt_{22}/(b't_{11}+bt_{22}), \tag{2.3b}$$

which ensure the normalization of the wave function and where t_{11} and t_{22} are transfer-matrix elements, which are taken to have values of unity.[21] The significance of the above wave function is that electron penetration into the barrier side, $In_{1-x}Al_xAs$ (B side), of the interface is taken into account.

The above envelope function obeys the Schrödinger equation given by

$$-\frac{\hbar^2}{2}\frac{\partial}{\partial z}\frac{1}{m(z)}\frac{\partial}{\partial z}\zeta(z)+V(z)\zeta(z)=E_0\zeta(z), \tag{2.4a}$$

where $m(z)$ is the position-dependent effective mass; i.e., $m(z)=m_B$ for $z<0$, and $m(z)=m_A$ for $z>0$. The heterojunction potential is given by

$$V(z)=V_0\phi(-z)+V_e(z), \tag{2.4b}$$

where $\phi(x)$ is a step function that is zero for $x<0$, or else it is unity, and V_0 is the potential barrier height. Here, $V_e(z)=V_s(z)+V_d(z)$, with the electron contribution to the potential given by

$$\frac{\partial}{\partial z}\epsilon(z)\frac{\partial}{\partial z}V_s(z)=-e^2N_s|\zeta(z)|^2, \tag{2.4c}$$

and the depletion charge contribution is obtained from

$$\frac{\partial}{\partial z}\epsilon(z)\frac{\partial}{\partial z}V_d(z)=-e^2[N_A(z)-N_D(z)], \tag{2.4d}$$

where $N_s=N/A$ is the areal electron density, $N_A(z)$,$N_D(z)$ are the position dependent acceptor and donor concentrations. The present model is convenient, for if we substitute Eq. (2.2) into Eqs. (2.4), we obtain analytic expressions for the heterojunction potential and ground-state energy level in terms of the variational parameters b and b'. One obtains

$$V_d(z)=e^2N_dz\left\{\frac{\phi(-z)}{\epsilon_B}+\frac{\phi(z)}{\epsilon_A}\right\}, \tag{2.5a}$$

for the depletion charge contribution to the potential, and

$$V_s(z)=V_{s<}(z)\phi(-z)+V_{s>}(z)\phi(z),$$
$$V_{s<}(z)=-(e^2N/\epsilon_B)B'^2(e^{b'z}-1)/b', \tag{2.5b}$$
$$V_{s>}(z)=-(e^2NB^2/\epsilon_A)\{e^{-bz}[bz^2+(4+2\beta)z+(6+4\beta+\beta^2)/b]-(6+4\beta+\beta^2)/b\},$$

for the electronic charge contribution to the potential. The energy level can be obtained by taking matrix elements of Eq. (2.4a) to obtain

$$E_0=\langle T\rangle_{00}+\langle V_d\rangle_{00}+\langle V_s\rangle_{00}+\langle V_0\rangle_{00}, \tag{2.6a}$$

$$\langle T\rangle_{00}=\frac{\hbar^2}{2}[(Bb)^2(1+\beta-\beta^2/2)/2m_A-(B'b')^2/4m_B],$$
$$\langle V_d\rangle_{00}=e^2N_d[-B'^2/b'\epsilon_B+B^2(6+4\beta+\beta^2)/b\epsilon_A], \tag{2.6b}$$
$$\langle V_s\rangle_{00}=e^2N[B'^2(1-B'^2/2)/b'\epsilon_B+B^4(33+50\beta+34\beta^2+12\beta^3+2\beta^4)/4b\epsilon_A],$$
$$\langle V_0\rangle_{00}=V_0B'^2.$$

The idea is to minimize the total energy[22] $E_T=E_0-\langle V_s\rangle_{00}/2$ with initial values of b and b' and iterate to convergence for a given concentration x and y in the $In_{1-x}Al_xAs/In_{1-y}Ga_yAs$ heterojunction alloy system. Reasonable starting guesses for b and b' are given by

$$b_{\text{initial}}\approx[12e^2m_A(N_d+11N/32)/\hbar^2\epsilon_A]^{1/3},$$
$$b'_{\text{initial}}\approx 2[2m_BV_0/\hbar^2]^{1/2},$$

with the first being the infinite barrier model case[23] and the second being the one suggested by Ando.[19] The temperature-dependent Fermi energy plays a role in our calculations; it is given by

$$E_F(T)=k_BT\,\mathrm{Ln}(\exp\{[E_F(0)-E_0]/k_BT\}-1)+E_0, \tag{2.7a}$$

where the zero-temperature Fermi level is

$$E_{F0}=\pi N_s\hbar^2/m_A+E_0. \tag{2.7b}$$

Finally, one notes that if in the above equations one lets $\beta\to 0$, the result will correspond to the infinite barrier heterojunction case in the electric quantum limit.[22]

B. Hamiltonian

The Hamiltonian for a two-dimensional interacting electron gas in the presence of scattering mechanisms, such as impurities (remote and background), polar optical (Frolich coupling), acoustic (via deformation potential), surface roughness, and alloy fluctuations, is written in the center-of-mass relative electron coordinate form[10-12] as mentioned previously. It is given by

$$H=H_c+H_e+H_{\text{ph}}+H_{e\text{-}i}+H_{e\text{-ph}}+H_{e\text{-sr}}+H_{e\text{-alloy}}, \tag{2.8}$$

where H_c is the contribution due to the center-of-mass part given by

$$H_c=\frac{\mathbf{P}^2}{2Nm_A}-eNE\mathbf{R}\ , \tag{2.9a}$$

and describes the coupling of the electric field with the center-of-mass coordinates in the x-y direction defined by $\mathbf{P}\equiv\sum_i\mathbf{p}_i$, $\mathbf{R}\equiv(1/N)\sum_i\mathbf{r}_i$, where, $\mathbf{P}\equiv(P_x,P_y)$, $\mathbf{R}\equiv(R_x,R_y)$, and N is the number of electrons in the conduction channel. The quantities $\mathbf{p}_i\equiv(p_{xi},p_{yi})$ and $\mathbf{r}_i\equiv(x_i,y_i)$ are the relative momentum and coordinate of the ith electron along the interface which are given in terms of the center-of-mass coordinates by $\mathbf{p}_i'=\mathbf{p}_i-\mathbf{P}/N$, $\mathbf{r}_1'=\mathbf{r}_i-\mathbf{R}$. The electron part of the Hamiltonian is written as

$$H_e=\sum_{k,\sigma}E_kC_{k\sigma}^\dagger C_{k\sigma}+\frac{1}{2}\sum_{\substack{k,k',q\\ \sigma,\sigma'}}V(q)C_{k+q,\sigma}^\dagger C_{k'-q,\sigma'}^\dagger C_{k'\sigma'}C_{k\sigma}\ , \tag{2.9b}$$

where $C_k^\dagger$ and C_k are creation and annihilation operators in the relative coordinates, and $V(q)$ is the electron-electron interaction potential, where image effects[24] have been neglected. The phonon part is given by

$$H_{\rm ph}=\sum_{Q,\lambda}\hbar\Omega_{Q\lambda}b_{Q\lambda}^\dagger b_{Q\lambda}\ , \tag{2.9c}$$

with $b_{Q\lambda}^\dagger$ and $b_{Q\lambda}$ the phonon creation and annihilation operators with wave vector $Q=(\mathbf{q},q_z)$ and branch λ. The quantity $\Omega_{Q\lambda}$ is the λth branch phonon-dispersion relation. The coupling of the relative electron coordinates with the impurities is described by

$$H_{e\text{-}i}(R)=\sum_{a,q,k,\sigma}\exp[iq\cdot(R-r_a)]u(q,z_a)C_{k+q,\sigma}^\dagger C_{k\sigma}\ , \tag{2.9d}$$

where $u(q,z_a)$ is the interaction potential between the relative electron and an impurity located at (r_a,z_a). The electron-phonon Hamiltonian is given by

$$H_{e\text{-ph}}=\sum_{q,q_z,\lambda}M(q,q_z,\lambda)e^{iq\cdot R}(b_{Q\lambda}+b_{-Q\lambda}^\dagger)C_{k+q,\sigma}^\dagger C_{k\sigma}\ , \tag{2.9e}$$

where $M(q,q_z,\lambda)$ is the electron-phonon interaction matrix element for the λth branch. The interaction between the electrons and the interface roughness is written as

$$H_{e\text{-sr}}(R)=\sum_{q,k,\sigma}\exp[iq\cdot R]V_{\rm sr}(q)C_{k+q,\sigma}^\dagger C_{k\sigma}\ , \tag{2.9f}$$

where $V_{\rm sr}(q)$ is the Fourier transform of the position-dependent potential fluctuation along the interface arising from less than perfect growth conditions.[5,18] Finally, the interaction between the electrons and the atomic fluctuations, due to alloying effects, is written as

$$H_{e\text{-alloy}}(R)=\sum_{i,q,k,\sigma}\exp[iq\cdot(R-r_i)]\Delta V(q,z_i)C_{k+q,\sigma}^\dagger C_{k\sigma}\ , \tag{2.9g}$$

where $\Delta V(q,z_i)$ describes the deviation of the atomic potentials from the average atomic potential of the alloy. This is modeled in the VCA.[20]

III. MOBILITY

A. Memory function

By defining a force operator, $\hat{F}_I$, in the Heisenberg representation as the commutator

$$\hat{F}_I\equiv d/dt\hat{P}_I(t)=-i[P(t),H]=NeE+\hat{F}\ ,$$

Ting and Nee[12] identified $\hat{F}$ as the force operator, due to the interaction Hamiltonian $H_i\equiv H_{e\text{-}i}+H_{e\text{-ph}}$. Further, by using a density-matrix formalism, and an expansion to lowest order in the interactions, in addition to averaging over the impurity coordinates, followed by a Laplace transformation and an average over the initial equilibrium density matrix, these authors obtained the memory function.[13] This memory function (zero frequency), appropriate to the work here, is given as a function of temperature by

$$M(T)=M_1(T)+iM_2(T)\ , \tag{3.1}$$

where M_2 is the imaginary part written as

$$M_2(T)=\frac{1}{Nm_A}\sum_q q_x^2\left[\int n_i(z_a)|u(q,z_a)|^2dz_a\right]\Pi_2'(q)-\frac{2\hbar}{k_BTNm_A}\sum_{q,q_z,\lambda}|M(q,q_z,\lambda)|^2q_x^2n'\left[\frac{\hbar\Omega_{Q\lambda}}{K_BT}\right]\Pi_2(q,\Omega_{Q\lambda})+\frac{1}{Nm_A}\sum_q q_x^2\langle|V_{\rm sr}(q)|^2\rangle\Pi_2'(q)+\frac{1}{Nm_A}\sum_q q_x^2\left\langle\sum_i|\Delta V(q,z_i)|^2\right\rangle\Pi_2'(q)\ . \tag{3.2a}$$

The temperature-dependent mobility is obtained from

$$\mu(T)\equiv-1/M_2(T)\ . \tag{3.2b}$$

Above, $n'(x)$ is the derivative of the phonon number with respect to x, Π_2 is the imaginary part of the density-density correlation function, and Π_2' is its derivative with respect to energy $\hbar\omega$ and evaluated at $\omega\rightarrow0$. $M_1(T)$ can be obtained by the use of the Kramers-Kronig relation.

The function Π_2 used here has been detailed in earlier work.[14] The function Π_2' is given by

$$\Pi_2'(q)=\frac{\Pi_{02}'(q)}{|1-V(q)\Pi_{01}(q)|^2}\ , \tag{3.3a}$$

where $V(q)$ is the electron-electron interaction potential given below, and

$$\Pi_{01}(q)=-\frac{m_A A}{2\pi\hbar^2}h(\varphi,\varphi_F)\ ,$$
$$\Pi_{02}'(q)=-\frac{AE_F}{\pi\hbar^4 k_F^2 q}\left[\frac{2m_A^5}{k_B T}\right]^{1/2}g'(\varphi-\varphi_F)\ , \tag{3.3b}$$

$$g'(y)\equiv\int_0^\infty\frac{\exp(y+z)}{[\exp(y+z)+1]^2 z^{1/2}}dz\ ,$$
$$\varphi\equiv(q/2k_F)^2\varphi_F,\quad \varphi_F=\frac{E_F}{k_B T}\ , \tag{3.3c}$$

and the limiting form of Π as $T\to 0$ is given in Ref. 12.

B. Matrix elements

The electron-electron interaction has the analytic form

$$V(q)=\frac{e^2}{2A\epsilon_{\rm ave}q}H(q)\ , \tag{3.4a}$$

with $\epsilon_{\rm ave}=(\epsilon_A+\epsilon_B)/2$ and overlap

$$H(q)=\frac{B'^4 b'}{b'+q}+\frac{2(BB')^2 bb'}{(b+q)(b'+q)}\left[\frac{2b^2}{(b+q)^2}+\frac{2b\beta}{b+q}+\beta^2\right]$$
$$+\frac{B^4 b}{(b+q)}\left[\frac{8b^2+9bq+3q^2}{2(b+q)^2}(1+2\beta+2\beta^2)\right.$$
$$\left.+\beta^3\left[\frac{2(2b+q)}{b+q}+\beta\right]\right]\ . \tag{3.4b}$$

This potential enters the mobility through the density-density correlation function in the random-phase approximation.

The electron-impurity interaction is given by

$$u(q,z_a)=\int_{-\infty}^{\infty}\varphi(q,z,z_a)|\zeta(z)|^2 dz\ , \tag{3.5a}$$

where the potential φ is obtained from Ref. 25. An approximate form for the ground state can be written as

$$\varphi(q,z,z_a)=\frac{Ze^2}{2\epsilon_{\rm ave}Aq}\left[e^{-q|z-z_a|}\right.$$
$$\left.-\frac{S_0 e^{-q|z-z_0|}e^{-q|z_0-z_a|}}{q+S_0}\right]\ , \tag{3.5b}$$

where z_0 is the value of z at which the envelope function is a maximum, and

$$S_0=\frac{e^2 N}{2A\epsilon_{\rm ave}E_{d0}}\ ,$$
$$E_{d0}=k_B T\left[1+\exp\left[\frac{E_F-E_0}{k_B T}\right]\right]\ . \tag{3.5c}$$
$$\times\mathrm{Ln}\left[1+\exp\left[\frac{E_F-E_0}{k_B T}\right]\right]\ .$$

Putting Eq. (3.5a) into the integral in the first term of Eq. (3.2), with the use of Eq. (2.2), one gets the impurity contribution in the form

$$\int n_i(z_a)|u(q,z_a)|^2 dz_a$$
$$=\left[\frac{Ze^2}{2Aq}\right]^2[(N_I A/\epsilon_B^2)K(q,s)+(n_i A/\epsilon_A^2)J(q)]\ , \tag{3.5d}$$

where the first term is due to the contribution from remote impurities located at a distance s away from the interface in the $In_{1-x}Al_xAs$ alloy side. The second term is due to background impurities. The functions $K(q,s)$ and $J(q)$, not shown, are analytic functions of q that depend on the parameters b and b'.

The phonon matrix element that appears in the second term of the memory function is written as

$$\sum_\lambda|M(q,q_z,\lambda)|^2=\sum_\lambda[|M_B(Q,\lambda)|^2|I_B(iq_z)|^2$$
$$+|M_A(Q,\lambda)|^2|I_A(iq_z)|^2]\ , \tag{3.6a}$$

where λ runs over the longitudinal polar optical, and acoustic-phonon contributions. The overlap terms are given by

$$|I_B(iq_z)|^2=\frac{B'^2 b'^2}{b'^2+q_z^2}\ ,$$
$$|I_A(iq_z)|^2$$
$$=\frac{B^4 b^2[b^4(\beta^2+2\beta+2)^2+2b^2 q_z^2\beta^3(\beta+2)+q_z^4\beta^4]}{(b^2+q_z^2)^3}\ , \tag{3.6b}$$

obtained by the use of Eq. (2.2), $I(iq_z)=\int_{-\infty}^{\infty}\exp(q_z z)|\zeta(z)|^2 dz$. The polar optical coupling strengths[26] are given by

$$|M_{A,B}(Q,\mathrm{PO}_l)|^2=\frac{e^2}{2\epsilon_{A,B}Q^2 V}\left[\frac{K_{A,B}}{K_{\infty,A,B}}1\right]\hbar\Omega_{0,A,B}\ , \tag{3.6c}$$

for the longitudinal phonon. Further, the transverse PO phonon contribution needs to be included[27] by

$$|M_{A,B}(Q,\mathrm{PO}_T)|^2=\frac{D_{A,B}^2\hbar}{2d_{A,B}\Omega_{A,B}V}\ , \tag{3.6d}$$

where $D=d_0/a$ is a deformation potential, and a is the lattice constant.[26] The acoustic-phonon deformation-

potential term is

$$|M_{A,B}(Q,\mathrm{DF}_l)|^2=\frac{\hbar\sigma^2_{A,B}Q}{2d_{A,B}v_{sl,A,B}V}\ . \tag{3.6e}$$

In the above equations, the A and B contributions correspond to the channel, $In_{1-y}Ga_yAs$, and barrier, $In_{1-x}Al_xAs$, sides of the heterojunction, taken into account within the VCA for concentrations x and y of Al and Ga, respectively, as discussed below.

The interface roughness contribution is obtained with the help of previous works,[5,18,23,28] so that one writes

$$V_{\mathrm{sr}}(q)=\frac{1}{2\pi}\sum_i V_{\mathrm{sr}}(r_i)\exp(-iq\cdot r_i)\ ,$$
$$V_{\mathrm{sr}}(r)=\Delta(r)\int_{-\infty}^{\infty}dz|\zeta(z)|^2\frac{\partial V}{\partial z}\ , \tag{3.7a}$$

where $V=V_s(z)+V_d(z)$ of Eqs. (2.5) and $\Delta(r)$ is the slow variation of the interface between the channel and barrier alloy materials. The final result is found to be in the form

$$\langle|V_{\mathrm{sr}}(q)|^2\rangle=\frac{\pi\gamma^2\Delta^2\Lambda^2}{A}\exp\left[-\frac{q^2\Lambda^2}{4}\right]\ , \tag{3.7b}$$

where Δ is the mean-square deviation of the height of the interface, and Λ is the lateral correlation length. In performing the average of the above quantity, the approximation

$$\langle\Delta(r)\Delta(r')\rangle=\Delta^2\exp\left[-\frac{|r-r'|^2}{\Lambda^2}\right]\ , \tag{3.7c}$$

due to Prange and Nee[29] has been made. The quantity γ in Eq. (3.7b) is given by

$$\gamma=\frac{e^2B'^2}{\epsilon_B}\left[N_d-\frac{B'^2N}{2}\right]+\frac{e^2B^2}{\epsilon_A}(\beta^2+2\beta+2)\left[\frac{B^2N}{2}(\beta^2+2\beta+2)+N_d\right]\ . \tag{3.7d}$$

The alloy scattering contribution in the last term of Eq. (3.2) is found with the help of the literature.[6–8,30,31] The unaveraged scattering potential is written in the form

$$\Delta V(q,z)=a\Delta V_q|\zeta(z)|^2,\quad \Delta V_q=(V_{A,B}-\bar{V}_{A,B})\ , \tag{3.8a}$$

where a is the lattice constant of the alloy A (channel side) or B (barrier side). The configurational averaged quantity to be used in the memory function is obtained in the form

$$\left\langle\sum_i|\Delta V(q,z_i)|^2\right\rangle=\frac{R_B^3}{A}[x(1-x)\delta_B^2B'^2b']+\frac{R_A^3}{4A}[y(1-y)\delta_A^2B^2b(2\beta^4+4\beta^3+6\beta^2+6\beta+3)]\ , \tag{3.8b}$$

where $R_{A,B}$ is the primitive cell radius of the alloys and

$$\delta_A\equiv V_{\mathrm{InAs}}-V_{\mathrm{AlAs}},\quad \delta_B\equiv V_{\mathrm{InAs}}-V_{\mathrm{GaAs}}\ , \tag{3.8c}$$

where the V's are the conduction-band minima of each compound.[19] In obtaining Eq. (3.8b), the VCA has been used.[20,30]

C. Virtual-crystal approximation

In order to obtain the various parameters used in the present work appropriate to compositions x and y in the systems $In_{1-x}Al_xAs$ and $In_{1-y}Ga_yAs$, the VCA is used.[20] In general if one lets Q be the quantity to be determined in a binary alloy j, where j can take on the values A and B for the materials $In_{1-x}Al_xAs$ and $In_{1-y}Ga_yAs$ with respective concentrations C_A and C_B, then the quantity Q is obtained using the expression

$$Q_j=(1-C_j)Q_{j1}+C_jQ_{j2}\ , \tag{3.9a}$$

at concentration C_j of the jth alloy. The quantities Q_{j1} and Q_{j2} are the values for the compounds 1 and 2 that make up the jth binary alloy. Thus, for the case of $In_{1-x}Al_xAs$, $j=A$, $j1=$InAs, $j2=$AlAs, and $C_A=x$, etc.

IV. RESULTS

The calculations performed in this work make use of band-structure parameters available in the literature[32–41] for the parent compounds InAs, AlAs, and GaAs and are given in Table I. For the $In_{1-x}Al_xAs$ alloy, the Γ point using a VCA approach is determined as a function of Al concentration and temperature[34,35] by

$$E_{\Gamma B}=(0.42+2.03\times10^{-4}\ \mathrm{T}+x[2.63-1.3\times10^{-4}\ \mathrm{T}])\ \mathrm{eV}\ . \tag{4.1a}$$

The X point follows

$$E_{XB}=(2.1-2.03\times10^{-4}\ \mathrm{T}+x[0.26-4.64\times10^{-4}\ \mathrm{T}])\ \mathrm{eV}\ . \tag{4.1b}$$

The $In_{1-y}Ga_yAs$ material has a direct band gap, which is approximated by

TABLE I. Parameters (Refs. 30–37) used throughout the calculations.

Quantity	GaAs	InAs	AlAs
E_Γ (eV)	1.52	0.42	3.05
E_X (eV)	1.98	2.1	2.36
a (Å)	5.64	6.06	5.66
K	13.18	14.55	10.06
K_∞	10.9	12.3	8.16
m (m_e)	0.067	0.023	0.15
d (gr/cm^3)	5.36	5.67	3.76
σ (eV)	7.0	−5.2	3.76
$\hbar\Omega_0$ (eV)	36.25	30.2	31.49
v_{sl} ($\times10^5$ cm/s)	4.71	4.41	5.65
V (eV)	1.52	0.42	2.36
d_0 (eV)	277.5	232.5	282.75

$$E_{\Gamma A}=(0.42-2.03\times10^{-4}\ \mathrm{T} +y[1.10-1.14\times10^{-4}\ \mathrm{T}])\ \mathrm{eV}\ . \quad (4.1c)$$

One of the desirable characteristics of the present system is that the band gap can be tuned so that $In_{1-x}Al_xAs$ is a direct band-gap barrier material, in which case the Al concentration has lower and upper limits, $x_d<x<x_c$, obtained from above as

$$x_c=\frac{1.68}{2.37+3.34\times10^{-4}\ \mathrm{T}}\ ,\qquad x_d=\frac{y[1.10-1.14\times10^{-4}\ \mathrm{T}]}{2.63-1.3\times10^{-4}\ \mathrm{T}}\ . \quad (4.2)$$

For $T=300$ K and $y=0.5$, this model gives $0.21<x<0.68$. Initially, $x=0.48$, and $y=0.47$ so that a comparison with experiment[40,41] can be made. The barrier height can be estimated using t e above results along with the 60:40 rule for band offsets[38,42] as

$$V_0\approx(1-0.4)(E_{\Gamma B}-E_{\Gamma A}) =(1.58-7.8\times10^{-5}\ \mathrm{T})x-(0.66-6.84\times10^{-5}\ \mathrm{T})y\ , \quad (4.3)$$

where it is assumed that $x<x_c$. Additionally, the remote impurities are located at a distance $s=80$ Å away from the interface,[43] within the barrier with a concentration $N_I=1.56\times10^{12}$ cm^{-2}, and the background impurity density is $n_I=1\times10^{15}$ cm^{-3}. The mean-square deviation of the interface height $\Delta=4$ Å, and the lateral correlation length $\Lambda=15$ Å. Also, the use is made of the following units: the energy is in units of $E_b\equiv me^4/2\hbar^2(4\pi\epsilon)^2=5.25$ meV, wave vector $k_b=(2mE_b/\hbar^2)^{1/2}=9.61\times10^7$ m^{-1}, and the temperature in units of $T_b\equiv E_b/K_b=60.9$ K, using the GaAs values.

Figure 1 shows the heterojunction potential obtained in the model of Sec. II. The potential (in units of E_b) and ground-state electron density are shown versus z (in units of $1/k_b$) for $T=0$, 77, and 300 K, for $N=1\times10^{12}$ electrons.

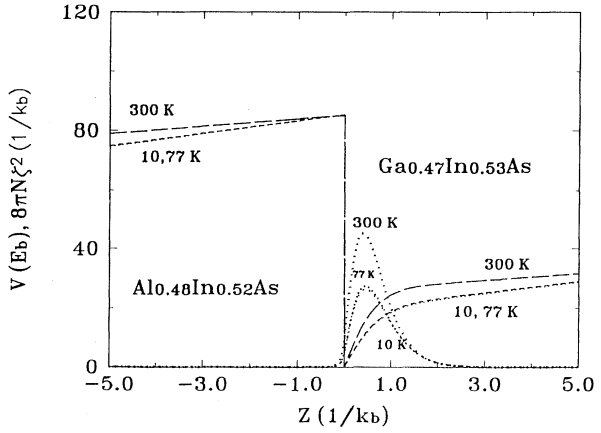

FIG. 1. Heterojunction potential in units of E_b versus distance z in units of $1/k_b$. The electron is also shown in units of $1/k_b$ for $N=1\times10^{12}$ electrons.

Figures 2(a) and 2(b) show the obtained variational parameters b and b' (in units of $1/k_b$) as well as the energy level (in units of E_b) versus Al concentration, where the Ga concentrations is $y=0.47$. Both figures show that the results for these parameters are slightly nonlinear functions of Al concentration, and show a strong dependence on the electron concentration.

Figure 3 shows the memory function (in units of $1/\tau_b$) versus temperature in units of T_b for all scattering contributions included. The total memory function shown is a composite of its individual contributions. In this figure, each scattering term is not temperature independent; however, the polar optical (transverse and longitudinal) are the dominant contribution above about 90 K. At lower temperature, it is the alloy, and the impurity contributions which limit the mobility, as will be seen in the figures discussed below in the low-temperature regime.

For low temperatures, the acoustic phonons also play a role, but in the present system their magnitude along with the surface-roughness contribution is not as significant as the alloy and impurity terms. The temperature behavior of the impurity scattering has been previously discussed in Ref. 12. At very low temperature the memory function contribution, due to acoustic phonons

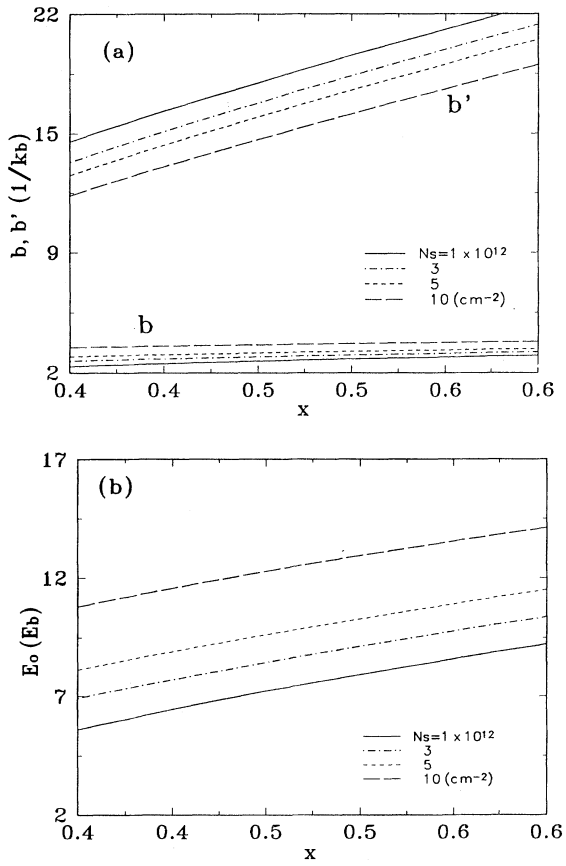

FIG. 2. (a) Variational parameters in units of $1/k_b$ versus Al concentration for various electron densities. (b) Ground energy in units of $1/k_b$ versus Al concentration for various electron densities.

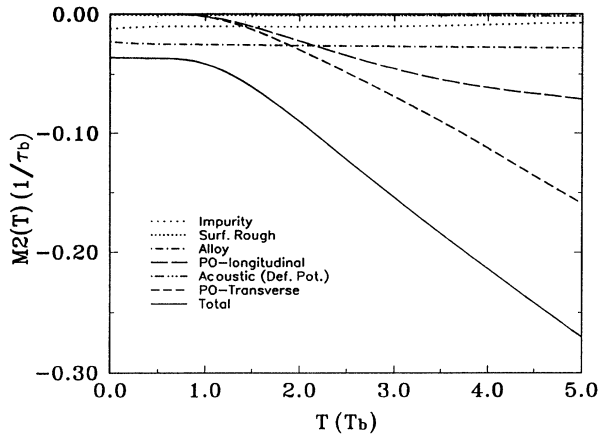

FIG. 3. The total memory function (solid line) in units $1/\tau_b$ versus temperature in units of T_b. The various scattering mechanisms' contribution to the memory function include impurity, PO-phonon, acoustic-phonon, interface roughness, and alloy fluctuations.

behaves according to the Bock-Gruneisen formula.[10] The spectra of an optical phonon and an acoustic phonon are quite different and the q dependence of their matrix element is responsible for their distinct behaviors.[26] Basically, at low temperatures, optical phonons can hardly be excited. At high temperatures, however, it is the optical phonons that are responsible for limiting the mobility. It should be mentioned that the results shown in Fig. 3 have been obtained with the experimental electron concentration of Kastalsky *et al.*,[40] shown in the inset of Fig. 4. Also shown in Fig. 4 is the mobility calculated using the memory function of Fig. 3. A comparison with the experimental work of Kastalsky *et al.*[40] and the work of Cheng *et al.*[41] has been carried out in this figure. We note that the results obtained are in very good agreement with the experimental result.

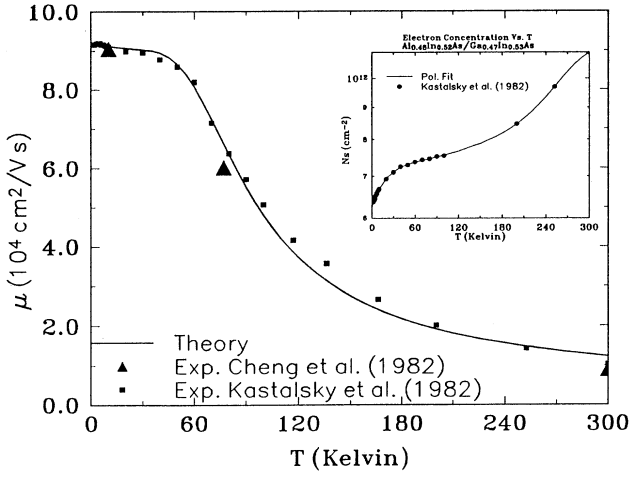

FIG. 4. The theoretical mobility versus temperature (solid line) is compared with the experimental data of Kastalsky *et al.* (Ref. 40) and Cheng *et al.* (Ref. 41). The inset shows the electron concentration as a function of temperature obtained from Ref. 40 and used in the performance of the mobility calculation.

In Fig. 5, the calculated mobility of $In_{1-x}Al_xAs/In_{1-y}Ga_yAs$ for $x=0.48$ versus Ga composition, y, is shown for $T=10$, 77, 300 K, using an electron concentration of $N_s=1\times10^{16}/m^2$. It should be noted that the mobility is greatest at low temperature and smallest at high temperatures in agreement with conventional wisdom. The mechanism responsible for limiting the mobility versus temperature in this figure is related with the discussion of Fig. 3 above. At low temperature, it is the alloy, the impurity, and to a smaller extent the interface roughness contributions that limit the mobility. This is the reason for the interesting behavior of the mobility versus Ga concentration. Of these contributions, the dominant term is due to alloy scattering due to fluctuations in alloy potentials. Thus, the mobility shown at 10 K is mainly limited by this term. At high temperatures, while the above terms still provide significant contributions, the polar optical phonons begin to become active in limiting the mobility as well. At the temperature of 300 K, the mobility shown in Fig. 5 is basically limited by the polar optical phonons. This is in concordance with our observations of the results presented in Fig. 3 in the high-temperature range.

Also noticeable in Fig. 5 is the nonlinear behavior of the mobility versus concentration; however, the trend of the mobility is to be high for the $In_{0.52}Al_{0.48}As/InAs$ system, and low for the $In_{0.52}Al_{0.48}As/GaAs$ system. This behavior is consistent with what would be expected if one thinks of the mobility as being proportional to the inverse of the effective mass of the system. Since InAs has a smaller effective mass than the GaAs system, this implies a higher mobility for the former.

Finally, in Fig. 6, the mobility for the $In_{1-x}Al_xAs/In_{1-y}Ga_yAs$ system for a fixed value of Ga composition, $y=0.47$, versus the Al concentration is shown for the same temperatures and parameters as in Fig. 5. The temperature dependence shown here has the same contributions as those included in Fig. 5. The behavior of the various mechanisms versus temperature

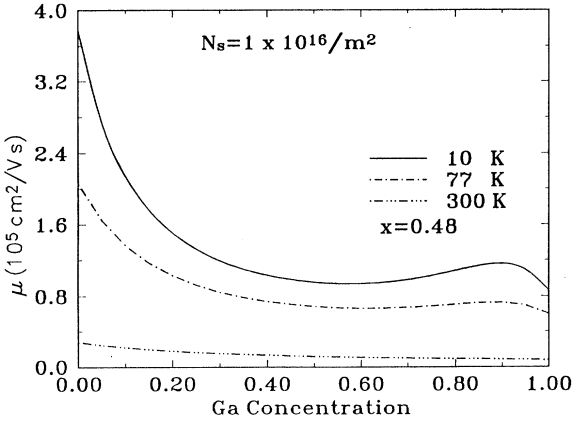

FIG. 5. The calculated mobilities for $In_{1-x}Al_xAs/In_{1-y}Ga_yAs$ versus y, for $x=0.48$, and temperatures of 10, 77, and 300 K. The scattering mechanisms included are as in Fig. 3. The electron concentration used is $N_s=1\times10^{16}/m^2$.

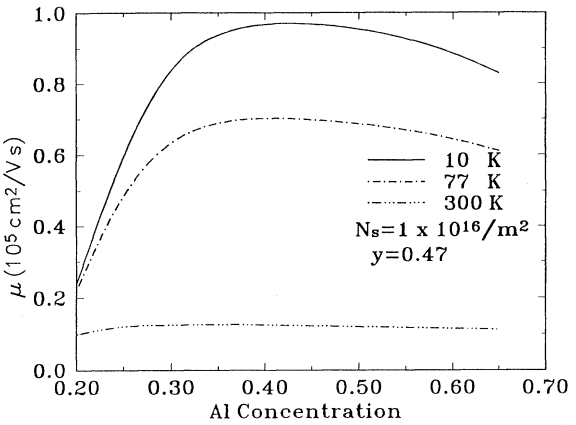

FIG. 6. The calculated mobilities for $In_{1-x}Al_xAs/In_{1-y}Ga_y$ versus x for $y=0.47$ and temperatures of 10, 77, and 300 K. The electron concentration used is as in Fig. 5 and scattering mechanisms as in Fig. 3.

and the relative strengths are similar to the previous discussions of Figs. 3 and 5. Here, the interesting feature that makes Fig. 6 unique is the fact that the concentration of Al varies, so that the heterostructure barrier changes in height. This is because $In_{0.8}Al_{0.2}As/In_{0.53}Ga_{0.47}As$ has a smaller barrier than does $In_{0.53}Al_{0.7}As/In_{0.53}Ga_{0.47}As$ system. For low Al concentration, the electrons are no longer confined to the $In_{1-y}Ga_yAs$ channel. Here, the electronic wave function has a significant penetration into what was supposed to be the barrier alloy material. Thus, the electrons are capable of sampling more scattering of the barrier material in addition to the scattering experienced in the high mobility channel. The net result is a decreased mobility for low Al concentration. Also since the intentional dopants are located in the barrier material, the electrons experience more impurity scattering in addition to alloy fluctuation scattering from the barrier material.

As the Al concentration rises, the mobility tends to increase relatively speaking, because the barrier height increases with Al concentration. There is a maximum mobility here, because the barrier effect is not the dominant effect beyond the peak point. What occurs next is similar to the behavior seen in Fig. 5. The electrons are mostly confined within the $In_{0.53}Ga_{0.47}As$ channel with some penetration into the barrier side. The small electron penetration has an electronic effective mass that is characteristic of $In_{0.3}Al_{0.7}As$. This effective mass is greater than that of the $In_{0.8}Al_{0.2}As$ system. By the same argument used in Fig. 5, the mobility, being inversely proportional to the effective mass, should decay in consistency with the behavior displayed in Fig. 6. Calculations below $x=0.2$ or above $x=0.7$ were not carried out, because of barrier and indirect band-gap transitions occurring near these values, respectively.

V. CONCLUSION

The electron mobility of a two-dimensional modulation-doped $In_{1-x}Al_xAs/In_{1-y}Ga_yAs$ heterojunction has been investigated within a memory-function theoretical framework. A variational wave-function model with penetration into the barrier side has been made use of. The theory incorporates various scattering mechanisms, due to polar optical and acoustic phonons, remote and background impurities, interface roughness, and alloy fluctuations. The strongest scattering mechanisms are due to alloy and impurity at low temperatures. For temperatures above 90 K, the polar optical phonons play a greater role in the scattering. A comparison with experiment yielded a very good agreement for the 0–300 temperature range studied. Further, the model has been used to obtain the mobility for the $In_{1-x}Al_xAs/In_{1-y}Ga_y$ system versus Al (with $y=0.47$) and Ga (with $x=0.48$) compositions for temperatures of 10, 77, and 300 K. Finally, the parameters used in the above alloy system have been obtained by the employment of the VCA with the appropriate input from the parent compounds, InAs, AlAs, and GaAs.

ACKNOWLEDGMENTS

The author was supported by a Cottrell College Science award of the Research Corporation. Computer support has been provided by a grant from the NSF-Pittsburgh Supercomputing Center. This research has been further supported by a West Georgia College Faculty grant.

[1]R. Dingle, H. L. Stormer, A. C. Gossard, and W. Wiegmann, Appl. Phys. Lett. **33**, 665 (1978).
[2]K. Inoue and T. Matsumo, Phys. Rev. B **47**, 3771 (1993).
[3]A. Kastalsky, R. Bhat, A. Y. Cho, and D. L. Sivco, J. Appl. Phys. **74**, 5259 (1993).
[4]K. S. Yoon, G. B. Stringfellow, and R. J. Huber, J. Appl. Phys. **63**, 1126 (1988); **62**, 1931 (1987).
[5]W.-P. Hong, J. Singh, and P. Bhattacharya, IEEE Dev. Lett. **EDL-7**, 480 (1986).
[6]W. Walukiewicz, H. E. Ruda, and H. C. Gatos, Phys. Rev. B **30**, 4571 (1984).
[7]P. K. Basu and B. R. Nag, Appl. Phys. Lett. **43**, 689 (1983).
[8]G. Bastard, Appl. Phys. Lett. **43**, 591 (1983).
[9]Y. Guldner, J. P. Vieren, P. Voisin, M. Voos, M. Razeghi, and M. A. Poisson, Appl. Phys. Lett. **40**, 877 (1982).
[10]X. L. Lei and C. S. Ting, Phys. Rev. B **36**, 8162 (1987); **30**, 4809 (1984); **32**, 1112 (1985); see, also, *Physics of Hot Electron Transport in Semiconductors,* edited by C. S. Ting (World Scientific, Singapore, 1992).
[11]C. S. Ting, S. C. Ying, and J. J. Quinn, Phys. Rev. B **14**, 4439 (1976).
[12]C. S. Ting and T. W. Nee, Phys. Rev. B **33**, 7056 (1986).
[13]W. Gotze and P. Wolfle, Phys. Rev. B **6**, 1226 (1972).
[14]J. E. Hasbun and T. W. Nee, Phys. Rev. B **44**, 3125 (1991); J. E. Hasbun, J. Phys. Chem. Solids **53**, 459 (1992).
[15]J. E. Hasbun, J. Appl. Phys. **75**, 270 (1994); J. Phys. Chem.

Solids **56**, 791 (1995).
[16]X. L. Lei, J. L. Birman, and C. S. Ting, J. Appl. Phys. **58**, 2270 (1985).
[17]X. L. Lei, J. Q. Zhang, J. L. Birman, and C. S. Ting, Phys. Rev. B **33**, 4382 (1986).
[18]T. Noda, M. Tanaka, and H. Sakaki, J. Cryst. Growth **95**, 60 (1989).
[19]T. Ando, J. Phys. Soc. Jpn. **51**, 3900 (1982).
[20]J. Hasbun, V. Singh, and L. Roth, Phys. Rev. B **35**, 2988 (1987); J. Hasbun and L. Roth, *ibid.* **37**, 2829 (1988), and references therein. The original VCA can be found in L. Nordheim, Ann. Phys. (Leipzig) **9**, 609 (1931); **9**, 641 (1931).
[21]T. Ando and S. Mori, Surf. Sci. **113**, 124 (1982).
[22]J. Hasbun, Phys. Rev. B **43**, 5147 (1991).
[23]T. Ando, A. B. Fowler, and F. Stern, Rev. Mod. Phys. **54**, 437 (1982).
[24]F. Stern and S. D. Sarma, Phys. Rev. B **30**, 840 (1984).
[25]K. Yokoyama and K. Hess, Phys. Rev. B **33**, 5595 (1986).
[26]P. Vogl, in *Physics of Nonlinear Transport in Semiconductors,* edited by D. K. Ferry, J. R. Barker, and C. Jacoboni (Plenum, New York, 1980), p. 75.
[27]K. Bhattacharyya, J. Appl. Phys. **75**, 4060 (1994).
[28]S. Mori and T. Ando, Phys. Rev. B **19**, 6433 (1979); T. Ando, J. Phys. Soc. Jpn. **43**, 1616 (1977).
[29]R. Prange and T. Nee, Phys. Rev. **168**, 779 (1968).
[30]N. F. Mott and H. Jones, *Theory of Metals and Alloys* (Dover, New York, 1958).
[31]A. Gold and A. Ghazali, Solid State Commun. **83**, 661 (1992).
[32]S. Adachi, J. Appl. Phys. **58**, R1 (1985).
[33]J. S. Blakemore, J. Appl. Phys. **53**, R123 (1982).
[34]M. Jaros, Rep. Prog. Phys. **48**, 1091 (1985).
[35]M. Neuberger, *Handbook of Electronic Materials: III-V Semiconducting Compounds* (Plenum, New York, 1971), Vol. 2.
[36]D. J. Wolford, W. Y. Hsu, J. D. Dow, and B. G. Streetman, J. Lumin. **18/19**, 863 (1979).
[37]R. Dingle, R. A. Logan, and J. R. Arthur, Jr., Inst. Phys. Conf. Ser. **33A**, 210 (1977).
[38]Y. Fu and K.A. Chao, Phys. Rev. B **43**, 4119 (1991).
[39]H. J. Lee, L. Y. Juravel, and J. C. Woolley, Phys. Rev. B **21**, 659 (1980).
[40]A. Kastalsky, R. Dingle, K. Y. Cheng, and A. Y. Cho, Appl. Phys. Lett. **41**, 274 (1982).
[41]K. Y. Cheng, A. Y. Cho, T. J. Drummond, and H. Morkoc, Appl. Phys. Lett. **40**, 147 (1982).
[42]T. W. Hichmott, in *Two-Dimensional Systems: Physics and New Devices,* edited by G. Bauer, F. Kuchar, and H. Heinrich (Springer-Verlag, New York, 1986), Vol. 67, p. 72.
[43]F. Stern, Appl. Phys. Lett. **43**, 974 (1983).